agriculture

MDPI

Article

Spatial and Temporal Variability of ET_o in Xinjiang Autonomous Region of China during 1957–2017

Yanhui Jia [1], Xiaojun Shen [2,3,*], Ruochen Yi [3] and Ni Song [1,*]

[1] Farmland Irrigation Research Institute, Chinese Academy of Agricultural Sciences, Xinxiang 453002, China
[2] School of Agricultural and Wine Sciences, Charles Sturt University, Wagga Wagga, NSW 2650, Australia
[3] College of Water Conservancy Engineering, Tianjin Agricultural University, Tianjin 300392, China
* Correspondence: shenxiaojun@tjau.edu.cn (X.S.); songni@caas.cn (N.S.); Tel.: +86-22-2386-8236 (X.S.); +86-373-339-3384 (N.S.)

Abstract: This article scientifically studies the direct impact of climate problems on the time transition of reference crop evapotranspiration in the Xinjiang Autonomous Region of China from 1957 to 2017, which is conducive to formulating irrigation scheduling and adaptive capacity countermeasures. The objective of this study is to investigate the impacts of climate change on ET_o for the cotton growing seasons. The meteorological data were collected from 48 meteorological stations in the region and analyzed using the Mann–Kendall test and linear trend. The results show the following points: (1) the ET_o decreases from low to high elevations, and with the increase in northern latitude. (2) The annual mean ET_o and average values of ET_o during the growing seasons for cotton exhibited two abrupt changes in the period 1957–2017, with the first abrupt change in 1995 to 1999 and the second abrupt change in 2006 to 2011. (3) The ET_o in Xinjiang of China demonstrates a decreasing trend during 1957–1996; a significant decreasing trend during 1997–2008; and a significant increasing trend during 2009–2017.

Keywords: climate change; ET_o; yield response factor; irrigation water requirement; cotton; Xinjiang

Citation: Jia, Y.; Shen, X.; Yi, R.; Song, N. Spatial and Temporal Variability of ET_o in Xinjiang Autonomous Region of China during 1957–2017. *Agriculture* **2022**, *12*, 1380. https://doi.org/10.3390/agriculture12091380

Academic Editor: Rabin Bhattarai

Received: 17 July 2022
Accepted: 30 August 2022
Published: 2 September 2022

1. Introduction

Much of the evidence from the past half century show that the increase in the global average temperature is mainly due to the increase in greenhouse gas emissions [1–3]. Global warming is a significant manifestation of the present observable and directly felt future climate change [4,5]. The period 2011–2015 was the hottest based on the previous records, about 0.57 °C higher than the reference temperature for the period of 1961–1990 [6]. Climate change is already affecting many aspects of life for people [7–9] and it will affect crop water demand [10,11], and the spatial and temporal redistribution of water resources in the future [12]. Reference crop water requirement (ET_o) is an important parameter for the calculation of crop water requirement [13–15]. In order to improve the efficiency of the irrigation water resources, it is important to study the spatiotemporal variation in ET_o under climate change.

In the past half century, China has produced many studies on regional temperature and rainfall [16,17]. However, there are relatively few studies on Northwest China against the background of continuous climate warming, and these are mainly focused on precipitation [18,19], air temperature [20], and small pan evaporation [21,22]. These studies showed the change feature of precipitation in Xinjiang as it changed from dry to wet in the middle and late 1980s, and the evapotranspiration potential showed a downward trend.

This study investigated the spatial transformation of ET_o in mountainous areas, oasis and desert areas of Xinjiang from 1957 to 2017. This scientific research plays an important role in revealing the fluctuation regularity of ET_o, mastering the evolution of drought and improving the utilization rate of irrigation water sources.

2. Materials and Methods

2.1. Description of the Xinjiang in the Northwest of China

Xinjiang is located in the most inland core of the Eurasian continent, with a longitude ranging from 73.40° E to 96.18° E and north latitude ranging from 34.25° N to 48.10° N and elevation of ranging from −155 m to 8611 m. It has a vast territory, with a total area of about 1.66 million hectares, accounting for more than 17% of China's land area. Tianshan, Altay and other mountains surround the Tarim Basin, Junggar Basin and other wide desert basins. The drought-stricken intermountain basins and humid and cold mountain areas are sensitive to climate issues [23]. Because it is far away from the surrounding deep sea, the arid climate is a very common inland continental climate, which is mainly affected by the inland drought norms, while the temperate monsoon climate in Asia is less harmful [24]. The annual average temperature is about 8 °C, and the annual average rainfall is less than 150 mm, slowly decreasing from north to south.

2.2. Data Processing

Continuous and long-time series of the observed daily maximum/minimum air temperature (T_{max}/T_{min}), relative humidity (Hr), wind speed at 10 m height (U_{10}) and global solar radiation (Rs) during 1957–2017 were collected from typical weather stations in Xinjiang (Figure 1). The FAO Penman–Monteith method used to calculate ET_o and can be shown in the following equation [25]:

$$ET_o = \frac{0.408\Delta(R_n - G) + \gamma \frac{900}{T_a+273} u_2(e_s - e_a)}{\Delta + \gamma(1 + 0.34u_2)} \quad (1)$$

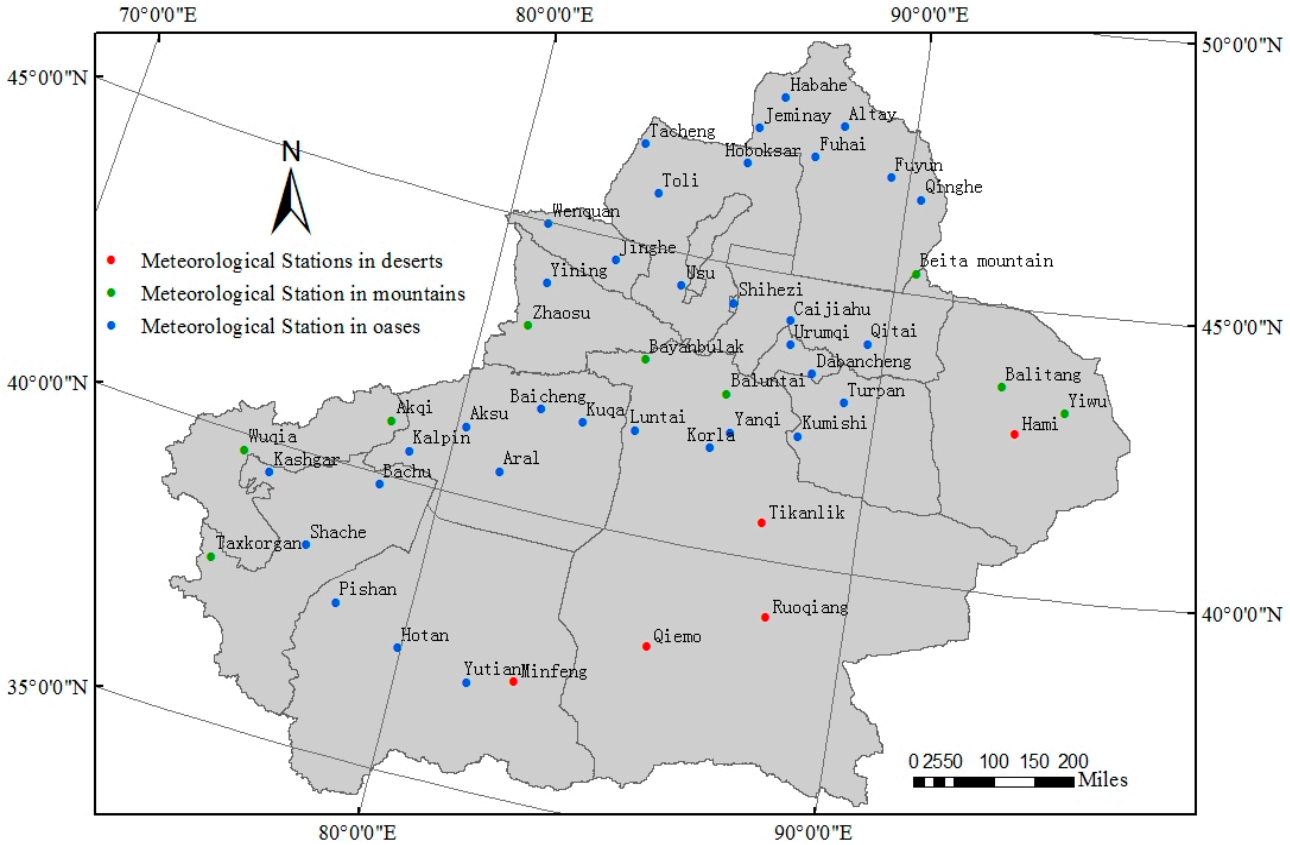

Figure 1. Xinjiang meteorological observation station is located in Northwest China.

In the above equation, ET_o is the reference evapotranspiration of crops (mm), R_n is the net radioactive material (MJ·m^{-2}·day^{-1}), G is the thermal diffusion coefficient of the soil

layer (MJ·m^{-2}·day^{-1}), γ is the air relative humidity constant (kPa·°C^{-1}), e_s is the saturated vapor pressure (kPa), e_a is the specific saturated vapor pressure (kPa), Δ is the slope of the saturated vapor pressure temperature curve (kPa·°C^{-1}), T_a is the daily mean temperature (°C) and u_2 is the daily mean wind speed at 2 m (m·s^{-1}).

The original daily temperature, air relative humidity, sunshine duration and wind speed data information are given by the National Climate Center of the China Meteorological Administration (NCC-CMA). The 48 meteorological stations selected in this study (Figure 1) have been maintained in accordance with the standards of the National Meteorological Administration of China. The standard requires strict quality control of the whole process before releasing the data information, including extreme inspections and regular inspections of duration consistency. For the oases, we chose large, medium and small urban meteorological stations located in densely populated areas to reflect the negative impact of human activities.

2.3. Methods

2.3.1. Mann–Kendall Method for Nonparametric Test

The nonparametric Mann–Kendall method used in climate trend analyses and gene mutation was created by Mann [26] and was changed by Kendall [27]. The Mann–Kendall method evaluates the development trend in the climate independent variable time series model, and has been widely used in the change trend, because it does not use the unique spread of data information samples [28].

In that way, H_o represents the distribution range of random variables, and H_1 represents the probability of double transformation. The test statistic S is obtained from the following formula:

$$S = \sum_{i=1}^{n-1} \sum_{k=i+1}^{n} \operatorname{sgn}(x_k - x_i) \tag{2}$$

where x_k and x_i are the sequential data values, n is the length of the data set, and

$$\operatorname{sgn}(\theta) = \begin{cases} +1, & \theta > 0 \\ 0, & \theta = 0 \\ -1, & \theta < 0 \end{cases} \tag{3}$$

If the sample size exceeds 10, the statistic S is basically normal, that is, the statistic is a normal random variable, and its expected value and standard deviation are as follows:

$$Z_C = \begin{cases} \frac{S-1}{\sqrt{var(S)}}, & S > 0; \\ 0, & S = 0; \\ \frac{S+1}{\sqrt{var(S)}}, & S < 0. \end{cases} \tag{4}$$

$$E(S) = 0 \tag{5}$$

$$var(S) = [n(n-1)(2n+5)]/18 \tag{6}$$

t represents the type of all given connections and Σ represents the number of all connections. In the Mann–Kendall test, another very useful technical index is the Kendall straight-line slope, which is the compressive strength with a monotonic development trend, which is calculated by the following formula:

$$\beta = Median\left(\frac{x_i - x_j}{i - j}\right), \quad j < i \tag{7}$$

In the above equation, $1 < j < i < n$. It indicates an "upward" trend, that is, it increases over time, and a negative value indicates a "downward" trend, that is, it decreases for a long time at any time.

2.3.2. Mann–Kendall's Method of Genetic Variation Test

Under zero assumption with the out trend, the time series of the variables do not change, and the time series can be regarded as $x_1, x_2, \ldots \ldots, x_n$. For each new item, m_i is calculated as the number of subsequent new items whose value in the coding sequence exceeds x_i. The test statistical analysis and calculation are as follows:

$$d_k = \sum_{i=1}^{k} r_k \quad (2 \le k \le N) \tag{8}$$

$$r_i = \begin{cases} 1\,, x_i > x_j \\ 0\,, x_i \le x_j \end{cases} \tag{9}$$

Assuming that the sequence is arbitrary and independent, the variance in the expected values $E(d_k)$ and d_k can be calculated as follows:

$$\begin{cases} E(d_k) = k(k-1)/4 \\ var(d_k) = \frac{k(k-1)(2k+S)}{72} (2 \le k \le N) \end{cases} \tag{10}$$

We can, therefore, obtain the statistic $u(d_k)$ with the following equation:

$$u(d_k) = (d_k - E(d_k))/\sqrt{var(d_k)} \tag{11}$$

The terms of the $u(d_k)$ $(1 \le k \le n)$ constitute curve C_1. If the normalized normal probability $\Pr(|u|) < |u(d_k)| > a$, the null hypothesis of no trend will be rejected at the confidence level a. The coding sequence of annual total precipitation applies the typical 95% confidence level. If this method is applied to the inverse level, it can obtain $\bar{u}$ (d_k), as shown in the following equation:

$$\begin{cases} \overline{u}(d_i) = -u(d_i) \\ i = n + 1 - i \end{cases} \cdots (i, i = 1,\ 2,\ 3,\ \cdots,\ n) \tag{12}$$

The terms of the $\bar{u}$ (d_k) $(1 \le k \le n)$ constitute another curve C_2. If C_1 exceeds the confidence line, it indicates that there is an important upward or downward trend in the coding sequence. If the intersection point of the C_1 and C_2 is between the two lines, we can conclude that climate gene mutations should be produced in this way [24].

2.3.3. Pre-Whitening Mann–Kendall Method

Pre-whitening [29] was proposed by von Storch (1995), and it was used to reduce the influence of serial correlation on the MK test. The formula is shown below.

$$Y_t = X_t - r \times X_{t-1} \tag{13}$$

where X_t represents the original sequential data values, Y_t represents the sequential data values without autocorrelation and r is the autocorrelation coefficient of the sequence data.

2.3.4. Trend-Free Pre-Whitening Mann–Kendall Method

By considering the influence of the dominant trend of the data series on the autocorrelation coefficient estimation, the method of removing the preset white trend is adopted to eliminate the influence of the trend on the autocorrelation coefficient estimation, and the MK test of the data series is more accurate. The procedure is as follows [29]:

$$X'_t = X_t - \beta \times t \tag{14}$$

$$Y'_t = X'_t - r \times X'_{t-1} \tag{15}$$

$$Y_t = Y'_t + \beta \times t \tag{16}$$

where β is the Kendall straight-line slope, which can be calculated by Formula (7), X_t' is the detrended series, Y_t' is the detrended series without autocorrelation and the Y_t series preserved the true trend without autocorrelation.

2.3.5. Two-Phase Linear Regression Model

The simple linear regression model with a change point is given as follows [30]:

$$X_i = \begin{cases} \alpha_1 + \beta_1 \times t_i + \varepsilon_1, & t_{min} \le t_i \le t_C \\ \alpha_2 + \beta_2 \times t_i + \varepsilon_2, & t_C \le t_i \le t_{Max} \end{cases} \quad (17)$$

where (X_i,t_i) are the observations that correspond to the dependent and the independent variables, α_1, α_2, β_1, β_2 are the regression coefficients with the usual interpretations, ε_1, ε_2 are the random error terms for each line of the regression model and the point t_C is the unknown change point.

C ($t_C \le C < t_C + 1$) and the other parameter values can be obtained by fitting, and the fitting formula is as follows:

$$X_i = \alpha_1 + \beta_1 \times t_i + \beta'(1 - C) \times INDc(t_i) + \varepsilon \quad (18)$$

$$\beta' = \beta_2 - \beta_1 \quad (19)$$

$$INDc(t_i) = \begin{cases} 0, & t_i \le C \\ 1, & t_i > C \end{cases} \quad (20)$$

Each regression coefficient is obtained by the least square method, and the sum of the squares of the residuals of the equation (S) is obtained; then, the significance test is carried out for the mutation trend. The statistic U calculation formula is as follows:

$$U = \frac{(S_0 - S)/3}{S/(n-4)} \quad (21)$$

In this equation, S_0 is the residual sum of squares of the linear regression equation without catastrophe and S is the residual sum of squares corresponding to the optimal mutation point. The mutation point was accepted at the significance level of 0.05, otherwise the mutation is not considered obvious. U is the F(3, $n-4$) distribution.

2.3.6. Dominant Analysis

Dominant analysis, also known as the advantage analysis method, was proposed by Budescu [31]. In order to analyze the relative importance of different influencing factors, firstly, it is necessary to carry out regression analysis on the dependent variables by various indicators (influencing factors) and different combinations of these indicators. Calculate the determination coefficient R^2 of the regression equation containing these indexes and various combinations of indexes, compare these R^2, and then analyze the improvement of R^2 after adding one index or a combination of indexes into the regression equation. The most improved indicators or combination of indicators are better than others. This method has the following two advantages: (1) it has model independence, that is, the relative importance of the prediction index is kept constant in each sub-model; (2) according to the relative importance of each prediction index, the total prediction variance in the regression model is decomposed and expressed as a percentage. Accordingly, the order of the influence of meteorological elements on ET_o can be realized.

3. Results and Discussion

3.1. Spatial Patterns of Annual Mean ET_o

The annual mean ET_o during 1957–2017 ranges from 660.94 mm to 1532.54 mm in Xinjiang, the ET_o ranges from 1532.54 mm to 660.64 mm with a latitude from 36.85° N to 45.93° N. It ranges from 660.64 mm to 1094.00 mm with a latitude from 43.03° N to 48.05° N (Figure 2a). The average value of ET_o for the cotton growing season during 1957–2017 ranges from 1108.15 mm to 519.01 mm with a latitude from 36.85° N to 44.96° N; the average value of ET_o ranges 519.01 mm to 870.30 mm, with a latitude from 43.03° N to 48.05° N (Figure 2a). The average value of ET_o for the cotton seedling stage during 1957–2017 ranges from 340.67 mm to 153.49 mm in Xinjiang; the average value of ET_o for the cotton squaring stage ranges from 224.82 mm to 105.15 mm, with a latitude from 36.85 to 48.05 degrees north latitude; the average value of ET_o for the cotton flowing-boll stage ranges from 431.79 mm to 209.29 mm, with a latitude from 36.85 to 48.05 degrees north latitude; the average value of ET_o for the cotton boll opening stage ranges from 110.87 mm to 50.92 mm, with a latitude from 36.85 to 48.05 degrees north latitude (Figure 2b). The value of the annual mean ET_o decreases with the values of the degrees for north latitude (Figure 2a,b); the value of annual mean ET_o for all years and the growing season of cotton increases with the values of the degree of elevation from 34.5 m to 935.0 m, and decreases with the degree of elevation from 935.0 m to 3090.1 m (Figure 2c,d).

High values of the annual mean ET_o in Xinjiang are found in deserts and the low values in mountainous areas (Figure 3). The average value of ET_o is found in different growth periods of the cotton area (Figure 3). The average value of ET_o in south Xinjiang is greater than that in north Xinjiang (Figure 3).

3.2. ET_o Change with Altitude and Elevation

The relationship between ET_o and relative height used to reveal the layout of ET_o conversion space is shown in Figure 2. The results show that ET_o is inversely proportional to latitude. The annual average ET_o decreases by 27.86 mm with the increase of 1° of the latitude, and the average ET_o in the cotton wadding growth season decreases by 8.21 mm with the increase of 1° of the latitude (Figure 2g,h). The results show that ET_o has vertical zonality; in other words, with the rise in altitude in Xinjiang, China, ET_o decreased significantly (Figure 2). The results show that ET_o is inversely proportional to altitude. The annual average ET_o decreases by 0.07 mm with the increase in altitude by 1 m, and the average ET_o in the cotton boll growing season decreases by 0.09 mm with the increase in altitude by 1 m (Figure 2i,j).

(**a**) (**b**)

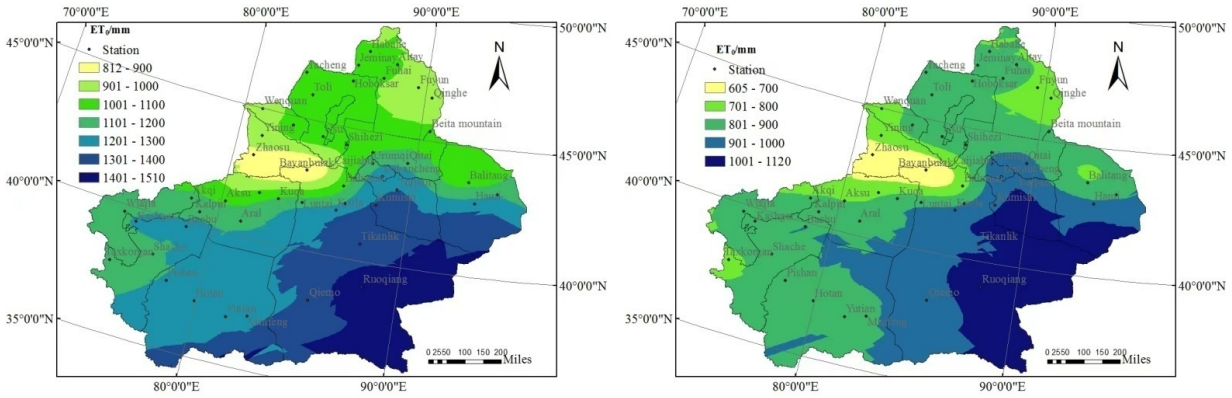

Figure 2. *Cont.*

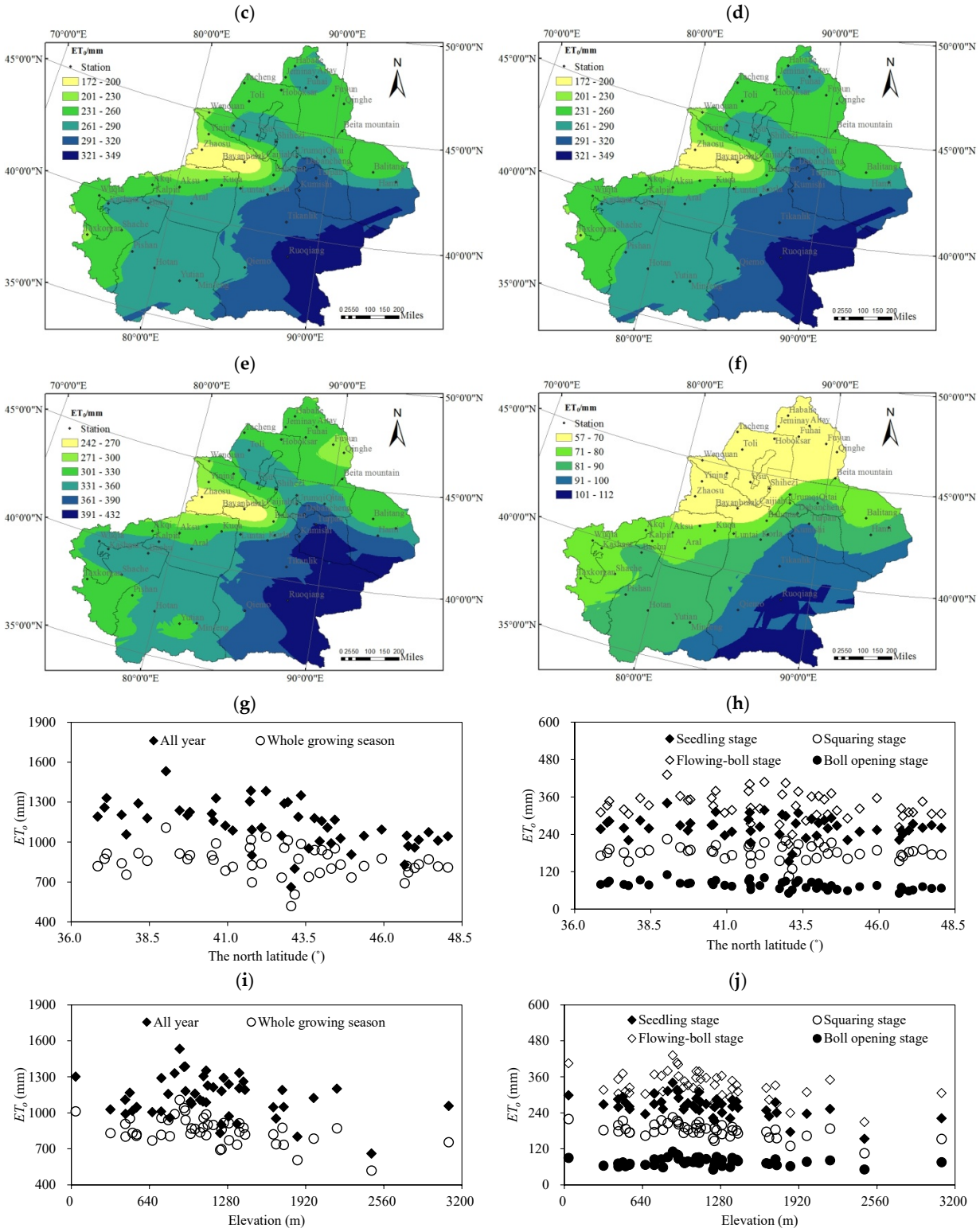

Figure 2. ET_o varies with space. (**a**): Annual average ET_o of Xinjiang; (**b**): the average ET_o value of the entire cotton growing season in Xinjiang; (**c**): the average ET_o value of cotton seedling stage in Xinjiang; (**d**): the average ET_o value of cotton squaring stage in Xinjiang; (**e**): the average ET_o value of cotton flowing-boll stage in Xinjiang; (**f**): the average ET_o value of cotton boll opening stage in Xinjiang; (**g**,**h**): relationship between the ET_o and latitude in Xinjiang; (**i**,**j**): relationship between the ET_o and elevation in Xinjiang of Northwest China.

3.3. ET_o Change with Precipitation

The relationship between the ET_o and the precipitation in Xinjiang is based on the long-term (1957–2017) meteorological data series during the cotton growing season (Figure 4). The results show that ET_o decreased with the increase in precipitation in the growing season for cotton in Xinjiang, the average ET_o decreases by 1.40 mm with the precipitation increase of 1 mm during the cotton growing season in Xinjiang (a), the average ET_o decreases by 1.57 mm with the precipitation increase of 1 mm during the cotton growing season in North Xinjiang (b), the average ET_o decreases by 1.42 mm with the precipitation increase of 1 mm during the cotton growing season in South Xinjiang (c), the average ET_o decreases by 1.24 mm with the precipitation increase of 1 mm during the cotton growing season in East Xinjiang and (d) the values of the correlation coefficient between rainfall and ET_o are −0.7245, −0.8241, −0.6065 and −0.5433. Figure 4 shows that the reference crop evapotranspiration rate in northern Xinjiang was highly affected by precipitation during the cotton growing seasons.

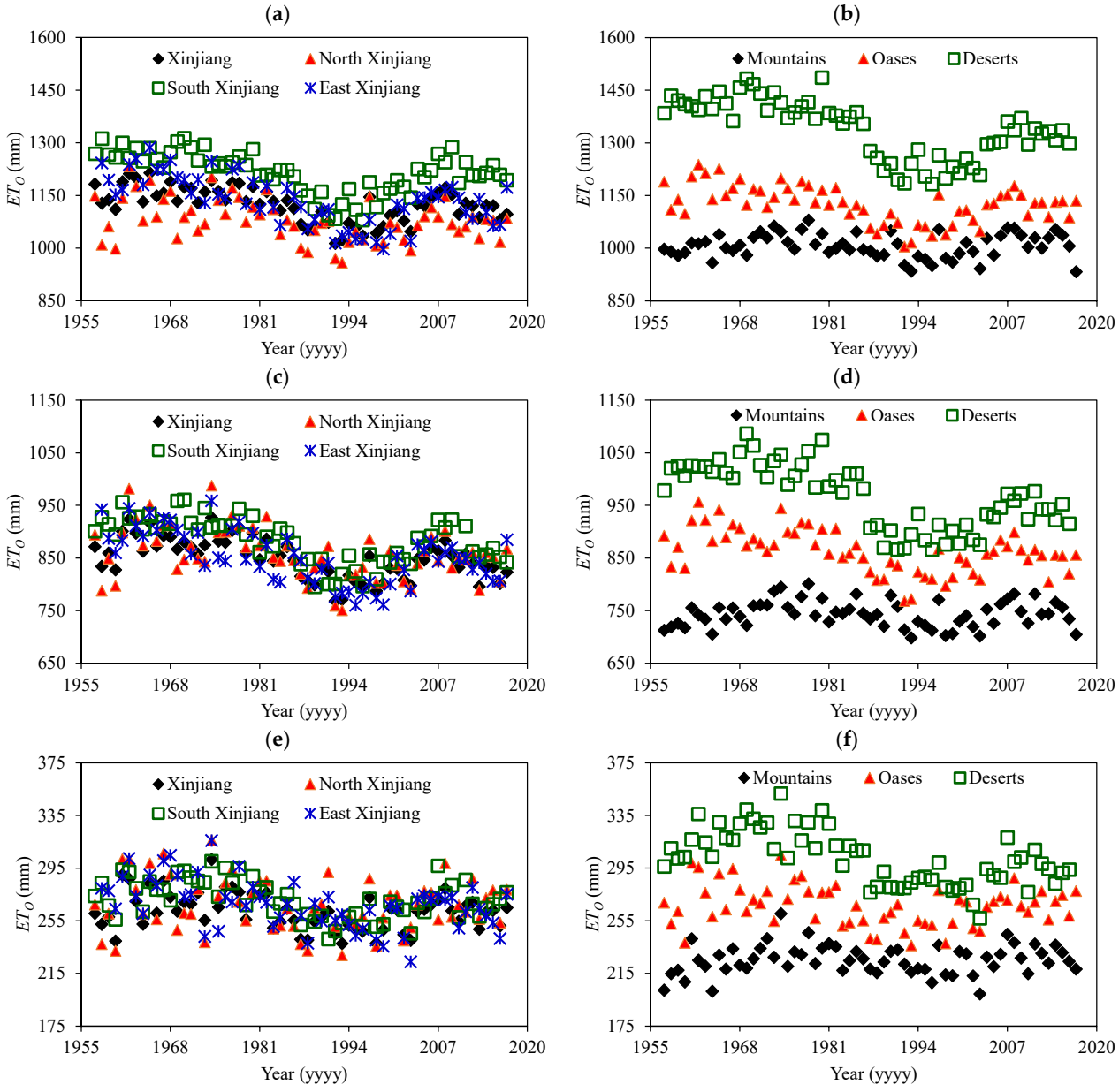

Figure 3. *Cont.*

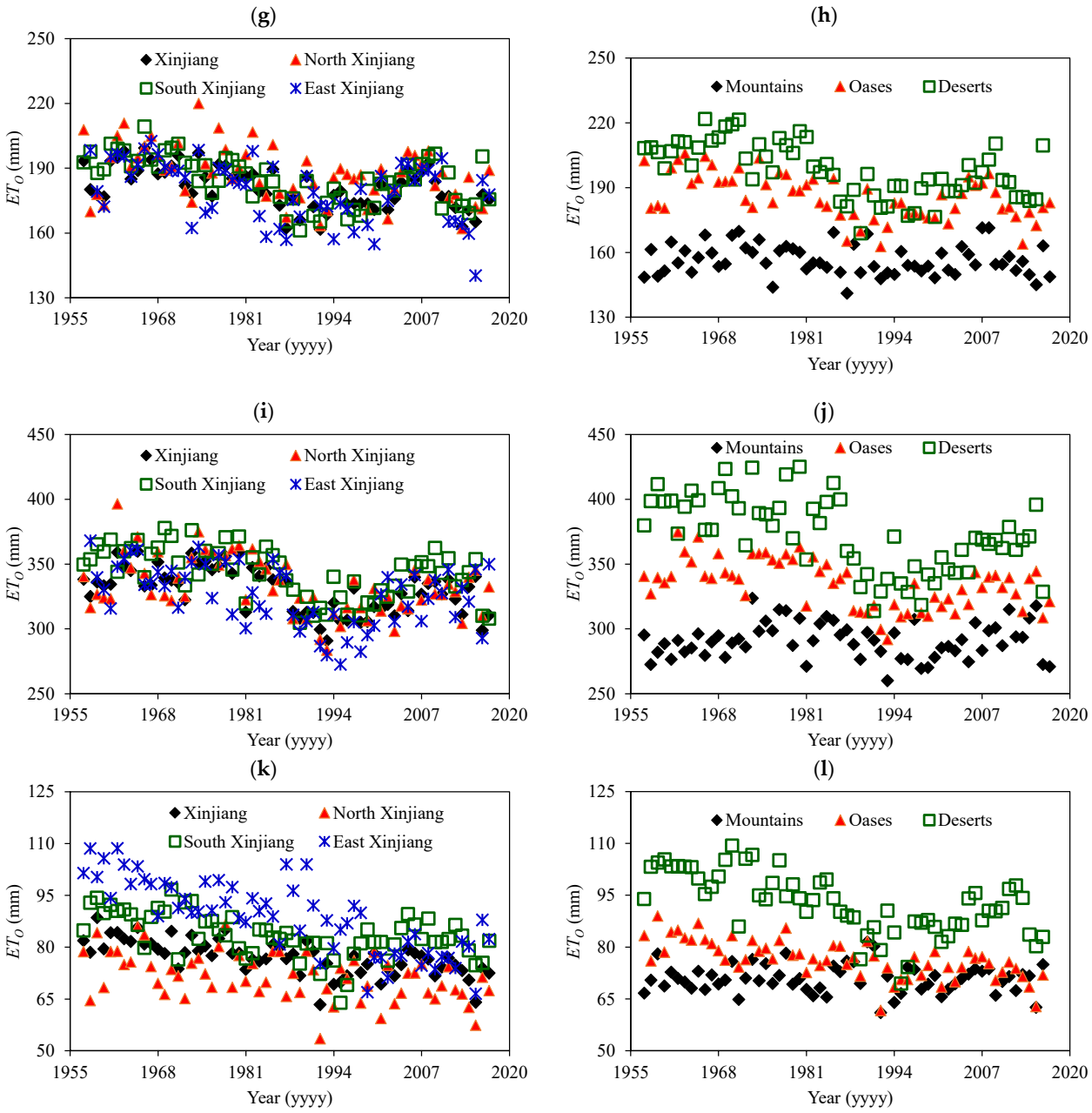

Figure 3. The change process of the ET_o in Xinjiang of Northwest China during 1957–2017. (**a**,**b**): Annual average ET_o over the entire year; (**c**,**d**): average ET_o value of cotton growing season; (**e**,**f**): average ET_o value of cotton seedling stage; (**g**,**h**): average ET_o value of cotton squaring stage; (**i**,**j**): average ET_o value of cotton flowing-boll stage; (**k**,**l**): average ET_o value of cotton boll opening stage.

The values of water consumption for cotton were directly affected by the change in ET_o and precipitation during the cotton growing season under the climate changes; furthermore, the irrigation water demand for cotton in Xinjiang was affected. If one considers the Shihezi region as an example, the value of K_c (crop coefficient) is 0.6 for cotton at Shihezi in northern Xinjiang [32], the values of water consumption for cotton were 124.65–554.58 mm during the growing seasons from 1957–2017, and the values of precipitation ranged from 50.5 mm to 235.4 mm, the values of irrigation water requirement for cotton ranged from 234.27 mm to 504.08 mm during the 1957–2017, and the irrigation water requirement decreased by 3.8 mm/10a during the 1950s–1990s, and increased by 1.84 mm/a during the 1990s–2010s.

Against the background of climate change, the contradiction between supply and demand of irrigation water for cotton in Xinjiang has become more serious.

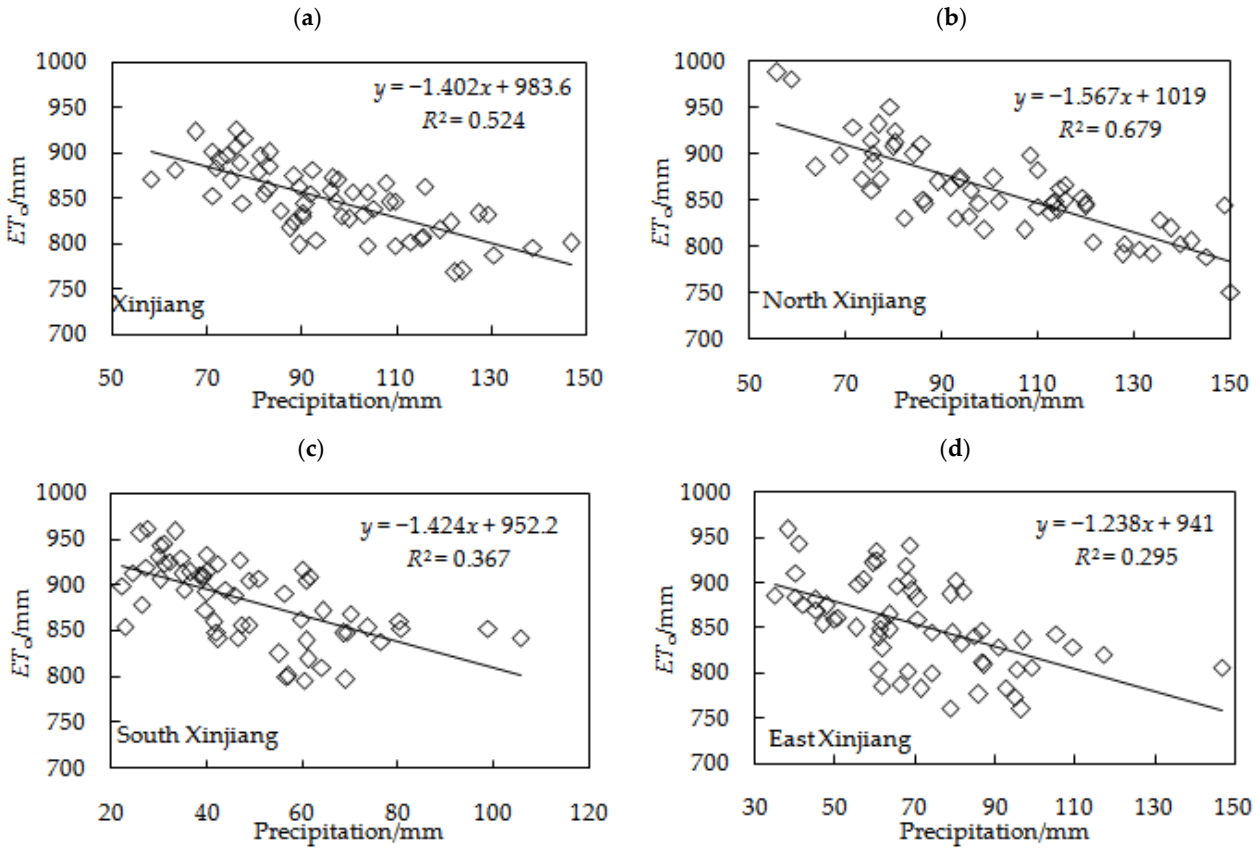

Figure 4. The relationship of the ET_o and the precipitation during the cotton growing seasons in Xinjiang. (**a**): Average value of Xinjiang; (**b**): Average value of North Xinjiang; (**c**): Average value of South Xinjiang; (**d**): Average value of East Xinjiang.

3.4. ET_o Change Trend

Through the autocorrelation test, it was found that almost all the ET_o series in Xinjiang show strong autocorrelation. Pre-whitening and trend-free pre-whitening are used to pre-process all the ET_o sequences. The typical treatment results are shown in Table 1. The results show that the two methods can effectively reduce the autocorrelation of the ET_o series, and the PW method is better than TFPW. However, the trend of the sequences processed by the PW method is seriously reduced. Therefore, the TFPW method is chosen to preprocess the sequences, and then the Mann–Kendall (m–k) nonparametric statistics is carried out. The Mann–Kendall (m–k) nonparametric statistical method showed that ET_o demonstrated a downward trend in general ($p < 0.01$).

The results of two-phase linear regression showed that the annual average ET_o in Xinjiang had a downward trend from 1957 to 1996 (Figure 5a), with a decline rate of 33.96 mm/10a; there was a significant growth trend from 1997 to 2008 (Figure 5a), with an annual growth rate of 71.41 mm/10a. From 2009 to 2017, there was an obvious downward trend (Figure 5b), with a decline rate of 66.64 mm/10a. Such growth trends are consistent with global and Chinese climate change [23,33].

Table 1. Mann–Kendall value and first-order coefficient of autocorrelation for original and two pre-whitening ET_o series.

Series	Average Value of ET_o during the Growing Seasons for Cotton				Annual Mean of ET_o			
	Xinjiang	North Xinjiang	South Xinjiang	East Xinjiang	Xinjiang	Mountains	Oases	Deserts
MK-original ET_o series	−4.3179	−2.7106	−4.4327	−4.4837	−3.8969	−0.1084	−3.0359	−5.3766
r1-Original ET_o series	0.6493	0.4124	0.7069	0.5870	0.6310	0.2817	0.5933	0.8346
MK-pre-whitening	−1.7539	−1.3968	−2.0473	−1.9708	−1.7157	−0.2487	−1.3840	−1.8560
r1-Pre-whitening	−0.1721	−0.0541	−0.3380	−0.1727	−0.1759	−0.0017	−0.1488	−0.1911
MK-trend-free pre-whitening	−4.6240	−2.9402	−5.0449	−4.5730	−4.3689	−0.3253	−3.0168	−6.7670
r1-Trend-free pre-whitening	0.3190	0.1580	0.2366	0.3092	0.2213	−0.0010	0.1514	0.5218

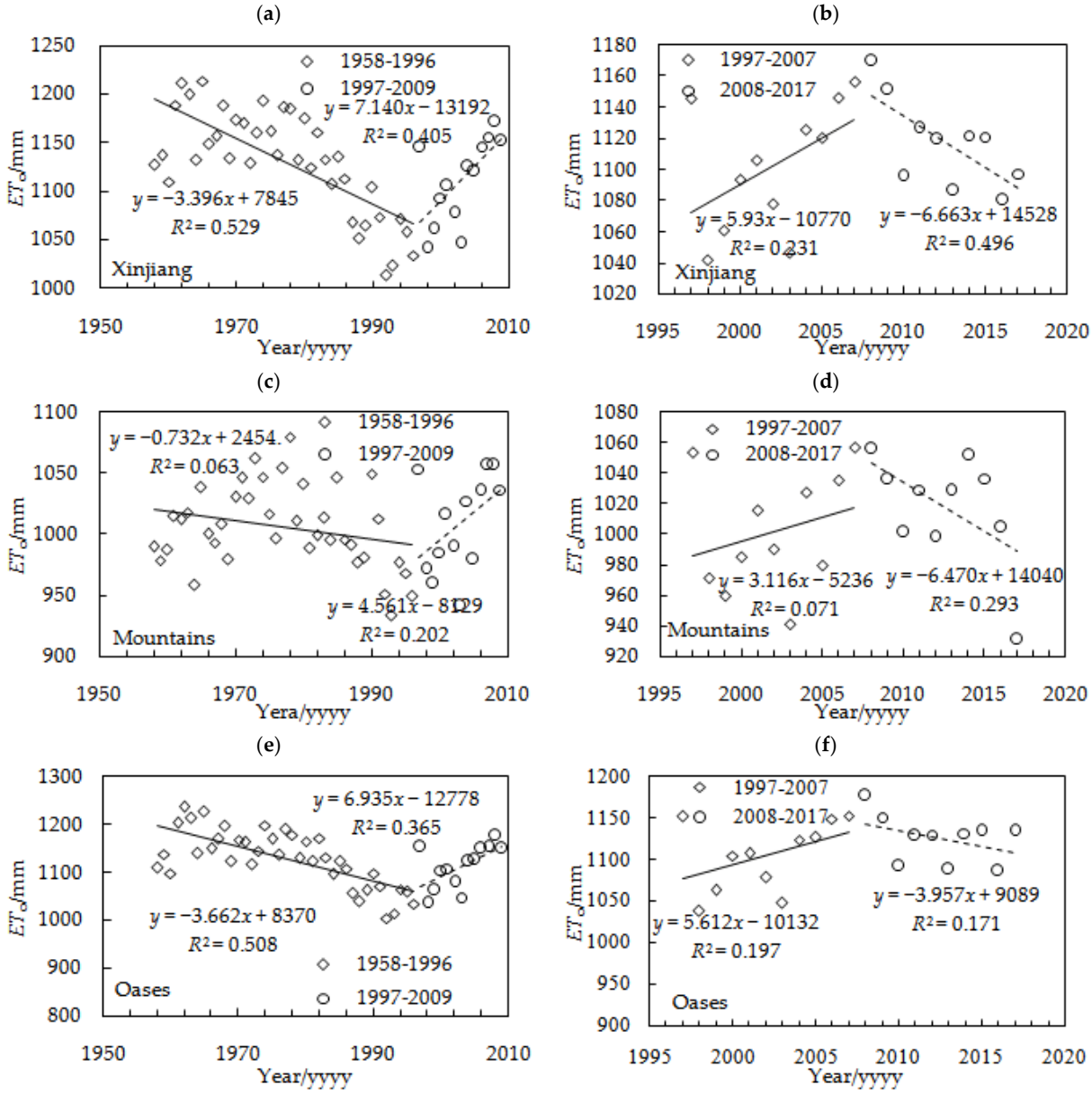

Figure 5. *Cont.*

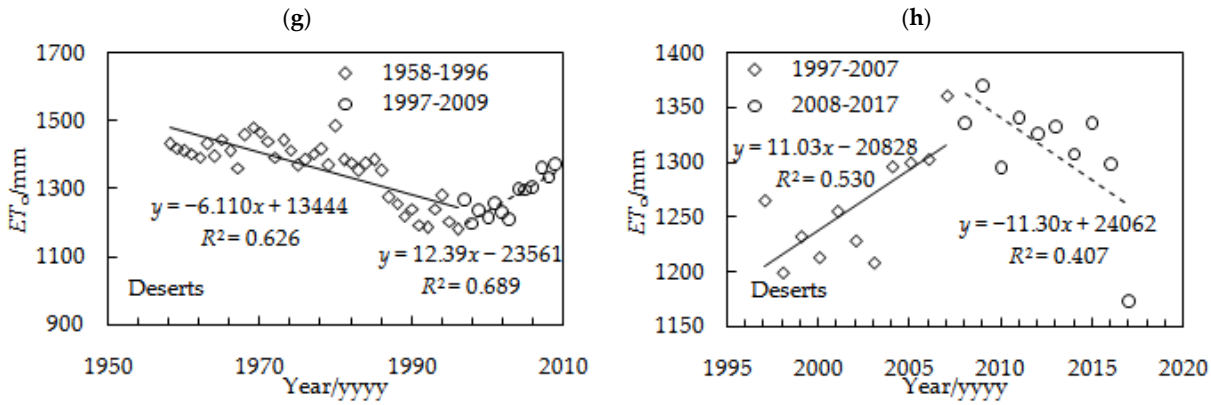

Figure 5. Abrupt change in annual mean ET_o in Xinjiang during 1957–2017. (**a**,**b**): Annual mean of ET_o in Xinjiang; (**c**,**d**): annual mean of ET_o in mountains; (**e**,**f**): annual mean of ET_o in oases; (**g**,**h**): annual mean of ET_o in deserts.

Figure 5 shows that the annual average ET_o mutation point occurred in Xinjiang in 1996 and 2008 (Figure 5a,b); for the oasis, it occurred in 1995 and 2008 (Figure 5e,f), followed by the mountain region in 1998 and 2010 (Figure 5c,d), and desert in 1999 and 2009 (Figure 5g,h); this is related to the unique geographical location and climatic condition garden landscapes. Because the mutation analysis shows that all garden landscapes and three specific garden landscapes have relative mutations around 1997 and 2009, we divide 60 years into the following three periods: before 1997, 1997–2009 and after 2009, and carry out a more detailed analysis of each link.

Among the three landscapes here, the mountainous area shows decreasing trends from 1957 to 1998 (Figure 5c), with a downward rate of 7.33 mm/10a, an upward trend from 1999 to 2010 (Figure 5c) with a rate of 45.62 mm/10a, and a downward trend from 2011 to 2017 (Figure 5d), with a downward rate of 64.71 mm/10a; the oases showed a downward trend from 1957 to 1995 (Figure 5e), with a speed of 3.63 mm/10a, an upward trend from 1996 to 2008 (Figure 5e) with a speed of 69.35 mm/10a, and a downward trend from 2009 to 2017 (Figure 5f), with a speed of 39.57 mm/10a; the desert showed a downward trend from 1957 to 1999 (Figure 5g), with a downward rate of 61.11 mm/10a, an upward trend from 1997 to 2009 (Figure 5g) with a rate of 123.99 mm/10a, and a downward trend from 2010 to 2017 (Figure 5h), with a downward rate of 113.05 mm/10a. The reasons for these trends mainly lie in the following two aspects: first, the ecosystem in the desert area has low stability and the mountain ecosystem has high stability; the other reason is that the Xinjiang has experienced rapid population growth, along with the fast expansion of urbanization, industrialization, and tourism. Human activity might have caused the differences among the different landscapes against the background of global warming and regional climate change.

Figure 6 shows that the ET_o gene mutation point of the cotton growing seasons in Xinjiang occurred in 1997 and 2008 (Figure 6a,b); the mutation point occurred in eastern Xinjiang in 1997 and 2006 (Figure 6g,h), in the south of Xinjiang in 1997 and 2007 (Figure 6e,f), and in the north of Xinjiang in 1997 and 2009 (Figure 6c,d); this is related to the unique geographical location and climatic conditions in different landscapes. Because the mutation analysis shows that all landscapes and three specific landscapes have relative gene mutations around 1997 and 2008, we divide 60 years into the following three periods: before 1997, 1997–2009 and after 2009, and carry out a more detailed analysis of each link.

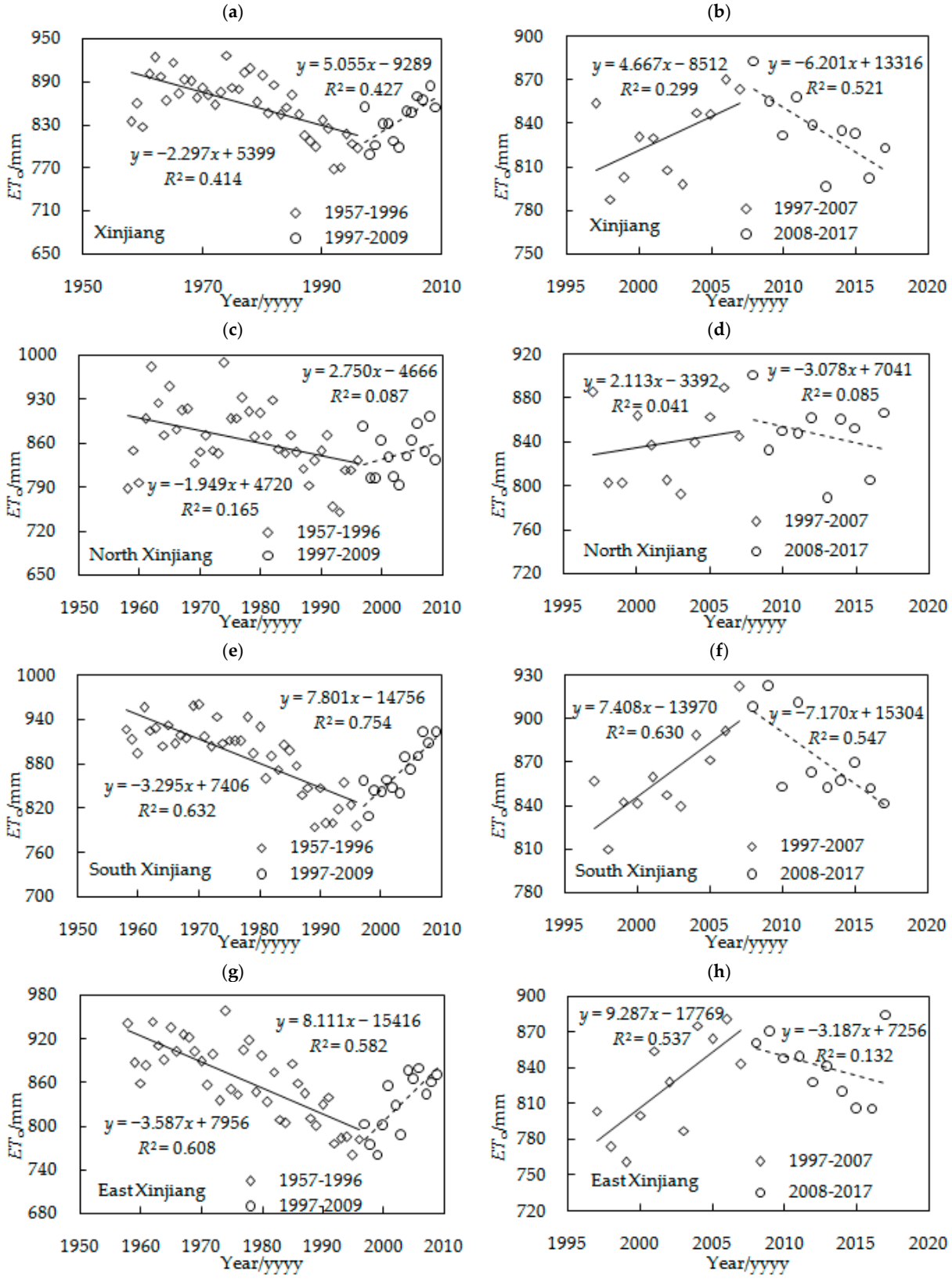

Figure 6. Abrupt change in average values of ET_o during the growing seasons for cotton in Xinjiang. (**a**,**b**): average value of ET_o during the growing seasons for cotton in Xinjiang; (**c**,**d**): average value of ET_o during the growing seasons for cotton in north Xinjiang; (**e**,**f**): average value of ET_o during the growing seasons for cotton in south Xinjiang; (**g**,**h**): average value of ET_o during the growing seasons for cotton in east Xinjiang.

The average values of ET_o during the growing season for cotton in Xinjiang showed a significant downward trend during 1957–1997 (Figure 6a), with a rate of 22.97 mm/10a, a significant upward trend during 1998–2008 (Figure 6a), with a rate of 50.53 mm/10a and a significant downward trend during 2009–2017 (Figure 6b), with a rate of 62.02 mm/10a. The average values of ET_o during the growing season for cotton in north Xinjiang showed a significant downward trend during 1957–1997 (Figure 6c), with a rate of 19.50 mm/10a, a significant upward trend during 1997–2009 (Figure 6c), with a rate of 27.51 mm/10a and a significant downward trend during 2010–2017 (Figure 6d), with a rate of 30.78 mm/10a. The average values of ET_o during the growing season for cotton in south Xinjiang showed a significant downward trend during 1957–1997 (Figure 6e), with a rate of 32.95 mm/10a, a significant upward trend during 1998–2007 (Figure 6e), with a rate of 78.01 mm/10a and a downward trend during 2008–2017 (Figure 6f), with a rate of 71.71 mm/10a. The average values of ET_o during the growing season for cotton in east Xinjiang showed a significant decreasing trend during 1957–1997 (Figure 6c), with a rate of 35.87 mm/10a, a significant increasing trend during 1998–2006 (Figure 6g), with a rate of 81.12 mm/10a and a decreasing trend during 2007–2017 (Figure 6c), with a rate of 31.88 mm/10a.

The cause of the ET_o change trend can be reduced to two main reasons, the first reason is the increase in irrigation and water conservancy after the founding of the People's Republic of China, which included increasing the irrigated area in Xinjiang and the regional air humidity; the second reason is the planting of windbreaks in agricultural areas that reduced the regional wind speed, finally leading to the continuous decline in the water requirement of reference crops from the 1950s to 1990s. Under the conditions of climate change, the temperature has been increasing since the 1990s, which explains why the values of ET_o during the cotton growing seasons showed an increasing trend from 1990s to 2010s.

3.5. Abrupt Change in ET_o

Two-phase linear regression analysis was used to analyze the abrupt trend of the ET_o time series, and the abrupt trend of each characteristic time point passed the significance level test of 0.05 ($F_{0.05}(3,48) = 2.80$, $F_{0.05}(3,16) = 3.24$). The Alar station (81.27° E, 40.55° N) was selected as an example to demonstrate the abrupt change in the time series of ET_o during the growing seasons for cotton (Figure 7). The results showed that the mutation occurred in 2001 and 2011. Using this method of detection, the abrupt changes in the annual average ET_o for the entirety of Xinjiang, southern Xinjiang, eastern Xinjiang, oasis and desert areas show obvious trends. For the average ET_o of the cotton growing season, there is a clear trend for Xinjiang, northern Xinjiang, southern Xinjiang, eastern Xinjiang and the oasis and desert areas.

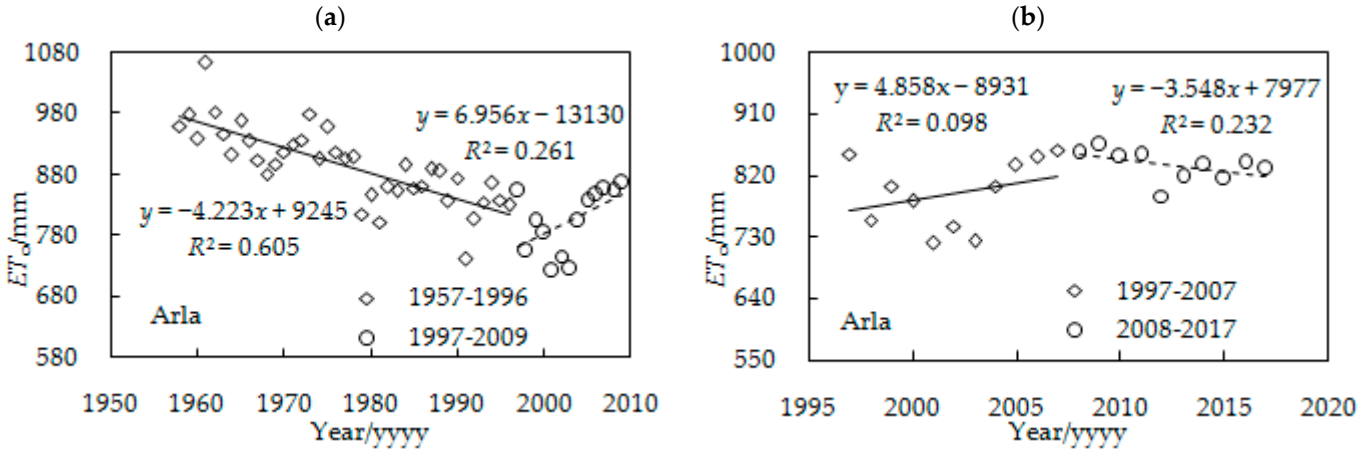

Figure 7. Abrupt change in average values of ET_o during the growing seasons for cotton in Arla of Northwest China. (**a**) The first mutation point; (**b**) The second mutation point.

The mutation age detected by the m-k method is shown in Figures 5–7. The results showed that in the past 60 years, the first mutation occurred in 1995–1999, and the second mutation occurred in 2006–2011 from 1957 to 2017. In this abrupt change year, due to climate change and human activities, vegetation cover underwent a great change. In 1987, the climate in Xinjiang changed from warm and dry to warm and humid, and the vegetation coverage changed [23]. In order to more effectively study the interaction between climate change, soil resource cover and human activities, we should understand the reasons for the sudden change in transpiration rate in Xinjiang.

4. Conclusions

The time specificity of ET_o in Xinjiang, China, from 1957 to 2017 was revealed by using the M-K nonparametric development trend and mutation detection, and two-phase linear regression model. The conclusions are as follows.

1. The annual average ET_o of the Xinjiang region demonstrates vertical zonality and longitude and latitude zonality. Due to the rise in altitude, it gradually decreases from high to low, and the ET_o changes significantly from southern Xinjiang to northern Xinjiang. For different garden landscapes, the low value of ET_o occurs in desert areas, and the low value consumption occurs in mountainous areas. The large-scale atmospheric circulation, location and altitude constitute complex standards that endanger the spatial distribution of the annual average transpiration rate in Xinjiang.

2. The results show that during the period from 1957 to 2017, ET_o showed a downward trend. The first mutation occurred in 1995–1999 and the second mutation occurred in 2006–2011. Among the three garden landscapes, ET_o decreases faster in desert areas, followed by oasis areas and the least in mountainous areas.

3. The results of the m-k analysis and two-phase linear regression show that 48 sites have experienced ET_o mutations, and the annual average of ET_o in Xinjiang, China, shows a downward trend from 1957 to 1996. There was also an obvious growth trend from 1997 to 2009 and a significant downward trend in the period from 2008 to 2017.

4. The annual average ET_o of Xinjiang demonstrates a sudden change, and Xinjiang, southern Xinjiang, eastern Xinjiang and the oases and desert areas show an obvious development trend. In terms of the average ET_o in the cotton growing season, there is an obvious trend for Xinjiang, northern Xinjiang, southern Xinjiang, eastern Xinjiang, the oases and desert areas. Because of the negative impact of human activities, the land resource cover in this area has changed greatly, so we must further study the relationship between land resource use and cover and ET_o change.

Author Contributions: Conceptualization, Y.J., X.S. and N.S.; methodology, X.S., Y.J. and N.S.; investigation, Y.J., X.S. and N.S.; data curation, Y.J. and N.S.; formal analysis, X.S., R.Y., Y.J. and N.S.; writing—original draft preparation, Y.J., X.S. and R.Y.; writing—editing, N.S. and X.S.; supervision, X.S. and N.S.; project administration, Y.J.; funding acquisition, Y.J. All authors have read and agreed to the published version of the manuscript.

Funding: This research was jointly supported by the National Natural Science Foundation of China (51790534), and the China Scholarship Council (No. 201703250034).

Institutional Review Board Statement: This study not involving humans or animals, so this research do not applicable.

Informed Consent Statement: This study involving humans, not applicable.

Data Availability Statement: Data involving meteorological data openly available in a public repository (the National Meteorological Information Center of China Meteorological Administration).

Acknowledgments: Thanks to the National Meteorological Information Center of China Meteorological Administration for offering the meteorological data. This study was supported by the Agricultural Science and Technology Innovation Program (ASTIP) of Chinese Academy of Agricultural Sciences. Special thanks are given to the anonymous reviewers for their constructive comments that improved this manuscript.

Conflicts of Interest: The authors declare no conflict of interest.

References

1. Solomon, S.D.; Qin, D.; Manning, M.; Chen, Z.; Miller, H.L. *Climate Change 2007-the Physical Science Basis: Working Group I Contribution to the Fourth Assessment Report of the IPCC*; Cambridge University Press: Cambridge, MA, USA, 2007.
2. Yoro, K.O.; Daramola, M.O. CO_2 emission sources, greenhouse gases, and the global warming effect. *Adv. Carbon Capture* **2020**, 3–28. [CrossRef]
3. Anderson, T.R.; Hawkins, E.; Jones, P.D. CO_2, the greenhouse effect and global warming: From the pioneering work of Arrhenius and Callendar to today's Earth System Models. *Endeavour* **2016**, *40*, 178–187. [CrossRef]
4. Thomas, J.; Brunette, M.; Leblois, A. The determinants of adapting forest management practices to climate change: Lessons from a survey of French private forest owners. *For. Policy Econ.* **2022**, *135*, 102662. [CrossRef]
5. Oertel, C.; Matschullat, J.; Zurba, K.; Zimmermann, F.; Erasmi, S. Greenhouse gas emissions from soils—A review. *Geochemistry* **2016**, *76*, 327–352. [CrossRef]
6. Kong, D.; Gu, X.; Li, J.; Ren, G.; Liu, J. Contributions of global warming and urbanization to the intensification of human-perceived heat waves over China. *J. Geophys. Res. Atmos.* **2020**, *125*, e2019JD032175. [CrossRef]
7. Lannelongue, L.; Grealey, J.; Inouye, M. Green algorithms: Quantifying the carbon footprint of computation. *Adv. Sci.* **2021**, *8*, 2100707. [CrossRef]
8. Lorenzoni, I.; Pidgeon, N.F. Public views on climate change: European and USA perspectives. *Clim. Chang.* **2006**, *77*, 73–95. [CrossRef]
9. Mcmichael, A.J.; Woodruff, R.E.; Hales, S. Climate change and human health: Present and future risks. *Lancet* **2006**, *367*, 859–869. [CrossRef]
10. Karimi, V.; Karami, E.; Keshavarz, M. Climate change and agriculture: Impacts and adaptive responses in Iran. *J. Integr. Agric.* **2018**, *17*, 1–15. [CrossRef]
11. Li, M.; Fu, Q.; Singh, V.P.; Ji, Y.; Liu, D.; Zhang, C.; Li, T. An optimal modeling approach for managing agricultural water-energy-food nexus under uncertainty. *Sci. Total Environ.* **2019**, *651*, 1416–1434. [CrossRef]
12. Luo, Q.; O'Leary, G.; Cleverly, J.; Eamus, D. Effectiveness of time of sowing and cultivar choice for managing climate change: Wheat crop phenology and water use efficiency. *Int. J. Biometeorol.* **2018**, *62*, 1049–1061. [CrossRef] [PubMed]
13. Ramanathan, K.C.; Saravanan, S.; Krishna, K.M.A.; Srinivas, T.; Selokar, A. Reference evapotranspiration assessment techniques for estimating crop water requirement. *Int. J. Eng. Technol.* **2019**, *8*, 1094–1100.
14. Djaman, K.; ONeill, M.; Diop, L.; Bodian, A.; Allen, S.; Koudahe, K.; Lombard, K. Evaluation of the Penman-Monteith and other 34 reference evapotranspiration equations under limited data in a semiarid dry climate. *Theor. Appl. Climatol.* **2019**, *137*, 729–743. [CrossRef]
15. Mirshekarnezhad, B.; Paknejad, F.; Amiri, E.; Ardakani, M.R.; Ilkaee, M.N. Functional strategies for certain growth stages of corn in response to environmental factors: Irrigation and planting date management. *Appl. Ecol. Environ. Res.* **2018**, *16*, 6169–6180. [CrossRef]
16. Qin, Y. *The Spatiotemporal Characteristics of Temperature Lapse Rate in China*; China University of Geosciences: Wuhan, China, 2021.
17. Xie, W.; Wang, S.; Yan, X. Evaluation on CMIP6 Global Climate Model Simulation of the Annual Mean Daily Maximum and Minimum Air Temperature in China. *Clim. Environ. Res.* **2022**, *27*, 63–78.
18. Tang, S. *Spatiotemporal Variations of the Temperature and Precipitation in Xinjiang during the Past 40 Years*; Si-chuan Normal University: Chengdu, China, 2021.
19. Xue, Y.; Han, P.; Feng, G. Change trend of the precipitation and air temperature in Xinjiang since recent 50 years. *Arid Zone Res.* **2003**, *20*, 127–130.
20. Yu, H.; Liu, J. Trend analysis of average temperature variations and runoff response in last 40 years in Xinjiang. *Water Power* **2007**, *22*, 169–177.
21. Hu, A.; Dong, X. A study on water surface evaporation in southern Xinjiang. *J. Arid Land Resour. Environ.* **2006**, *20*, 22–24.
22. Hu, A.; Guo, X. A model of water surface evaporation forecasting for Xinjiang plain area. *J. China Hydrol.* **2006**, *26*, 24–27+41.
23. Shi, Y.; Shen, Y.; Kang, E.; Li, D.; Ding, Y.; Zhang, G.; Hu, R. Recent and future climate change in northwest China. *Clim. Chang.* **2007**, *80*, 379–393. [CrossRef]
24. Liu, Q.; Yang, Z.; Cui, B. Spatial and temporal variability of annual precipitation during 1961–2006 in Yellow River Basin, China. *J. Hydrol.* **2008**, *361*, 330–338. [CrossRef]
25. Allen, R.; Pereira, L.; Raes, D.; Smith, M.; Allen, R.G.; Pereira, L.S.; Martin, S.; Allen, R.; Pereira, L.; Raes, D.; et al. *Crop Evapotranspiration: Guidelines for Computing Crop Water Requirements*; FAO Irrigation and Drainage Paper 56; Food and Agriculture Organization of the United Nations: Rome, Italy, 1998.
26. Mann, H.B. Non-parametric test against trend. *Econometrica* **1945**, *13*, 245–259. [CrossRef]
27. Kendall, M.G. *Rank Correlation Methods*; Hafner: New York, NY, USA, 1948.
28. Kahya, E.; Kalayc, S. Trend analysis of stream flow in Turkey. *J. Hydrol.* **2004**, *289*, 128–144. [CrossRef]
29. Sheng, Y.; Pilon, P.; Phinney, B.; Cavadias, G. The influence of autocorrelation on the ability to detect trend in hydrological series. *Hydrol. Processes* **2002**, *16*, 1807–1829.

30. Acitas, S.; Senoglu, B. Robust change point estimation in two-phase linear regression models: An application to metabolic pathway data. *J. Comput. Appl. Math.* **2019**, *363*, 337–349. [CrossRef]
31. Budescu, D.V. Dominance analysis: A new approach to the problem of relative importance of predictors in multiple regression. *Psychol. Bull.* **1993**, *114*, 542–551. [CrossRef]
32. Shen, X. *Water-Saving Mechanism and Optimal Irrigation Pattern for Effective Water Use and High-Quality of Cotton under Drip Irrigation*; Chinese Academy of Agricultural Sciences: Beijing, China, 2012.
33. Ren, G.; Xu, M.; Chu, Z.; Guo, J.; Ying, W. Changes of surface air temperature in China during 1951–2004. *Clim. Environ. Res.* **2005**, *10*, 717–727.